HIGH-RESOLUTION OPTICAL AND NEAR-INFRARED IMAGING OF YOUNG CIRCUMSTELLAR DISKS

MARK McCAUGHREAN
Astrophysikalisches Institut Potsdam

KARL STAPELFELDT
Jet Propulsion Laboratory, California Institute of Technology

and

LAIRD CLOSE
Institute for Astronomy, University of Hawaii

astrophysics
star formation
circumstellar matter

In the past five years, observations at optical and near-infrared wavelengths obtained with the Hubble Space Telescope and ground-based adaptive optics have provided the first well-resolved images of young circumstellar disks which may form planetary systems. We review these two observational techniques and highlight their results by presenting prototype examples of disks imaged in the Taurus-Auriga and Orion star-forming regions. As appropriate, we discuss the disk parameters that may be typically derived from the observations, as well as the implications that the observations may have on our understanding of, for example, the role of the ambient environment in shaping the disk evolution. We end with a brief summary of the prospects for future improvements in space- and ground-based optical/IR imaging techniques, and how they may impact disk studies.

I. DIRECT IMAGING OF CIRCUMSTELLAR DISKS

The Copernican demotion of humankind away from the center of our local planetary system also provided the shift in perspective required to understand its cosmogony. Once it was apparent that the solar system comprised a number of planets in essentially circular and coplanar orbits around the Sun, theories for its formation were developed involving condensation from a rotating disk-shaped primordial nebula, or Urnebel. The so-called "Kant-Laplace nebular hypothesis" eventually held sway in the latter half of the twentieth century after lengthy competition with rival "catastrophic" theories (see Koerner 1997 for a review), and was subsequently vindicated by the discovery of analogues to the Urnebel around young stars elsewhere in the galaxy.

These circumstellar disks were first detected indirectly, via infrared excess emission in spectral energy distributions (SEDs), polarization mapping, kinematic asymmetries in stellar winds, UV boundary layer emission, and the presence of bipolar collimated jets. These diverse observations could only be reconciled with each other by invoking a flattened disk of dust and gas around the young star, a model tied together with early evidence for molecular gas in Keplerian rotation around the young source HL Tau (see Beckwith and Sargent 1993 for a review).

However, direct images of circumstellar disks were sought in order to reinforce the paradigm more viscerally. The coronagraphic detection of an edge-on disk around the main sequence star β Pictoris (Smith and Terrile 1984) raised early hopes, but unfortunately, surveys of larger samples of nearby main sequence stars yielded no other disk images (Smith et al. 1992; Kalas 1996). This result is now understood to be a consequence of the especially large optical depth of the β Pic disk compared to other debris disk sources, and models show that, in general, disks are not expected to be detected around main sequence stars unless an order of magnitude improvement can be made in suppressing the stellar light in coronagraphic imaging (Kalas and Jewitt 1996). More recently, studies of the somewhat younger main sequence star HR 4796A have shown that debris disks with high enough optical depths can be imaged via direct emission from warm dust particles at thermal-IR wavelengths (Jayawardhana et al. 1998; Jura et al. 1998; Koerner et al. 1998), as well as in scattered light at near-IR wavelengths (Schneider et al. 1999).

However, there are important caveats concerning the β Pic and HR 4796A disks. They are relatively evolved, optically thin, effectively gas-free, consisting of only small amounts (a few lunar masses) of reprocessed dust, possibly replenished by collisions between much larger asteroids or planetesimals. Thus, while interesting in the context of later disk evolution after the main planet-building phase, they provide little insight into the nature of young, primordial disks. Also, at ~ 16 and 70 pc respectively, they are considerably closer than the nearest star-forming regions, making their structure relatively easy to resolve.

For more recently formed disks, there is a clear observational challenge: at the ~ 150 pc distance of the nearby low-mass star-forming regions such as Taurus-Auriga, our own 60 AU diameter solar system would subtend only 0.4 arcseconds, and only 0.1 arcseconds at the 500 pc distance to the Orion giant molecular clouds, the nearest site of ongoing high- and low-mass star formation. The knowledge that the young solar system was probably significantly larger, also encompassing a then optically-thick proto-Kuiper Belt, alleviates matters somewhat, but nevertheless, resolving even a several hundred AU diameter circumstellar disk at a distance of several hundred parsecs still requires subarcsecond spatial resolution.

The VLA provides this resolution at centimeter wavelengths, but emission from gas in thermal equilibrium in a disk at 10–50 K is impossible to detect until the millimeter/submillimeter regime is reached. Millimeter interferometer arrays including BIMA, OVRO, Plateau de Bure, and Nobeyama now provide $\sim$ arcsec resolution, giving indications of the density and velocity structure in disks in Taurus-Auriga (e.g., Mundy et al. 1996; Koerner and Sargent 1995; Guilloteau et al. 1997; Kitamura et al. 1997; Mundy et al., this volume; Wilner and Lay, this volume), while planned larger interferometer arrays will deliver 0.1 arcsecond resolution and better.

The same fiducial 0.1 arcsec resolution is the diffraction limit of 2.4-m telescope at 1 μm wavelength, which can now be achieved via space-based imaging with the *Hubble Space Telescope* (HST) and ground-based adaptive optics (AO). Although the bulk of the disk gas cannot be detected directly in emission at optical/near-IR wavelengths, the scattering and absorbing properties of the associated dust can be used to obtain images of the disk. This chapter reviews the following: how young disks can be seen at optical/near-IR wavelengths; the relative merits and demerits of the various imaging techniques; example objects, including edge-on disks where the central star is completely obscured, disks seen in silhouette against bright emission lines in H II regions, and disks where the central star or binary is clearly visible; the inferences that can be made as to the structure, mass, and evolutionary status of the disks; the influence of environment on the disks; and the impact of future instrumentation developments on the field.

II. DETECTABILITY AND TECHNIQUES

A. The detectability of disks at optical/near-IR wavelengths

Millimeter and thermal-IR observations image the gas and warm dust in a disk directly in emission, while optical/near-IR observations rely on either dust scattering or absorption. At these wavelengths, the scattering cross-section and opacity of typical dust grains is high, and by virtue of their high masses and densities, young circumstellar disks should be optically thick. Thus the full geometrical area of a young disk is available to scatter light from the central star(s) (from the top surface of the disk or from more tenuous dust in an associated envelope) or to be seen in absorption against a bright background.

Observations of scattered or absorbed starlight are much more sensitive to small amounts of dust than observations of emission at longer wavelengths. For typical ISM dust grains, a uniform surface density disk with radius 100 AU containing as little as a few Earth masses of gas and dust would still have an optical depth at visible wavelengths greater than unity. Thus, in principle, nebulosity can be seen around young stellar objects to a limiting mass hundreds of times smaller than currently achievable in millimeter continuum surveys. A caveat is that the central star is also bright at optical/near-IR wavelengths, generally presenting a severe contrast problem, as seen for the debris disks around main sequence stars. However, under favorable circumstances, the disk may be seen near edge-on, obscuring the star completely and leaving the disk clearly visible.

B. Imaging with the Hubble Space Telescope

Free from Earth's atmosphere, the HST has a diffraction-limited point spread function over an order of magnitude in wavelength ($\sim$2000Å–2 μm). This inherently stable, well-characterized PSF, combined with a clean optical train, high throughput, and low background, yields very deep, very high contrast images anywhere on the sky. However, the resolution of the 2.4-m diameter HST is ultimately limited compared with that of the current generation of 8–10 m ground-based telescopes.

C. Imaging with ground-based adaptive optics

On large ground-based telescopes, the spatial resolution is degraded by atmospheric seeing effects to the arcsecond level, significantly worse than the intrinsic optical/near-IR diffraction limit. Speckle techniques have long been used to retrieve diffraction-limited resolution for bright objects, employing post-detection processing of large numbers of very short exposure frames. Images of a small sample of very bright circumstellar disks around both young and evolved stars have been made in this way (e.g., Beckwith et al. 1984, 1989 for HL Tau; Falcke et al. 1996 for η Car; Osterbart et al. 1997 for the Red Rectangle).

Substantial improvement in dynamic range and sensitivity can be made using AO techniques. A relatively bright star (either the object of interest itself or a nearby companion) is monitored at high speed, allowing seeing-induced motions and distortions to be compensated for using a flexible mirror, yielding near diffraction-limited images in real-time, which can be further improved through post-detection deconvolution. AO techniques can be applied to the largest available ground-based telescopes, implying resolutions approaching 0.025 arcsec at 1 μm for 10-m class telescopes. Currently 0.1 arcsec resolution is routinely achieved at 2 μm on 4-m class telescopes.

Since a suitably bright nearby star must be available for wavefront sensing, sky coverage is limited, although in the specific case of young stellar objects (YSOs) within a few hundred parsecs, the source itself is usually bright enough to be used, as long as the disk is not seen edge-on. A more fundamental issue is the instability in the low-level halo surrounding the diffraction-limited core due to variable and imperfect correction: this is particularly problematic for studies of faint nebular emission around bright stars.

III. A MENAGERIE OF DISKS

In this section, we present a detailed discussion of the observations of a number of prototype disk systems with both the HST and ground-based AO. These are arranged according to how well the central star is suppressed, starting with edge-on systems where the star is unseen, moving to non-edge-on silhouette systems where the contrast of the disk can be enhanced using a narrow-band filter, and finishing with systems where the stars are bright enough to interfere with the interpretation of the disk structure.

A. Edge-on systems

Disks seen edge-on offer the best opportunity to study their structure, since the bright central star is not seen directly at optical/near-IR wavelengths. For a typical optically-thick flared disk with a scale height on the order of 10% of the radius, the central star will be occulted in about 10% of all possible viewing angles. Although several such sources are now known, their frequency of occurrence appears to be less than expected from these simple geometrical arguments, probably because current catalogues of young sources (e.g., optically-visible T Tauri stars) are biased against edge-on disk systems by definition. Also, since these systems, by definition, lack a bright central star, they are generally very difficult to study using speckle or AO techniques.

A defining characteristic of sources with edge-on disks is a bipolar reflection nebula structure, with two lobes of scattered light separated by a dark lane. These nebulae have sharp brightness gradients perpendicular to the lane, and show their greatest elongation in a direction parallel to it. In addition, edge-on disk sources are all relatively faint in the near-IR, have significant optical/near-IR polarization ($> 2\%$), and any associated jets lie close to the plane of the sky, and thus have low radial velocities. We now describe a number of template systems in order of evolutionary status.

1. IRAS 04302+2247: a disk forming within an extended envelope

IRAS 04302+2247 is a very young star embedded in the Taurus L 1536 molecular cloud. Lucas and Roche (1997) showed it to consist of a central dust lane and a bipolar reflection nebula, modelling the latter as a circumstellar envelope. More detailed near-IR images made using NICMOS on the HST (Fig. 1a; Padgett et al. 1999a) show the central dust lane to be sharply defined, with reddening at its edges clearly indicating increased density toward the midplane. The observed length of the dust lane suggests that a disk has formed, whose outer radius could be as much as 450 AU. Irregular bright and dark streamers within the two nebula lobes possibly indicate material infalling onto the disk. A rotating molecular gas structure has been resolved within the dust lane by millimeter interferometry (Padgett et al. 1999b), while millimeter continuum measurements imply a circumstellar mass $\sim 10^{-2}\,M_{\odot}$. Models including this disk mass yield a vertical extent consistent with the observed thickness of the dust lane. Thus the dust lane of IRAS 04302+2247 appears to trace a large, young disk, although a surrounding envelope structure remains essential to account for the infrared SED and the full extent of scattered light: therefore this source is likely at an early evolutionary stage.

2. Edge-on silhouette disks: Orion 182-413 and 114-426

The silhouette disks in the Orion Nebula are compact structures seen in absorption against the bright nebulosity of the H II region, and provide an important group of coeval disks for comparative studies. In most cases, the disk is not oriented edge-on and a young Trapezium Cluster star is seen at the center: these are discussed further in Section III.B. Two sources are seen edge-on however. Orion 182-413 (also known as HST 10; O'Dell & Wen 1994; Bally et al. 1998a) contains a dark absorption bar some 200 AU across seen within a larger bright globule, the latter being ionized by the OB stars at the center of the cluster. The presumed central star remains undetected even at $4\,\mu$m, and although no reflected continuum nebular lobes are seen, these would be difficult to detect against the bright ionized globule. Interestingly, the dark absorption bar is seen in emission in the v=1–0 S(1) line of H_2 at $2.122\,\mu$m (Chen et al. 1998), directly confirming the presence of molecular gas in the disk.

A clearer example is found in the much larger Orion 114-426. Optical HST images (McCaughrean & O'Dell 1996) show a dark, thick silhouette 1000 AU across, with faint continuum reflection nebulosities either side of the midplane. In the near-IR, the central star again remains undetected at least to $4\,\mu$m, and NICMOS images at 1–$2\,\mu$m show that the dust lane appears smaller and thinner, with the bipolar reflection nebulosities much brighter and more symmetric (Fig. 1b; McCaughrean et al. 1998). The long axis of the silhouette shrinks by 20% from 0.6–$1.9\,\mu$m, too small a change to be due to plausible intrinsic radial density gradients in the original disk structure; rather, abrupt truncation at some outer radius is required. The non-detection of the central star can be combined with disk models to yield a lower-limit disk mass of $5\times10^{-4}\,M_{\odot}$ (McCaughrean et al. 1998), while a comparison of the dust lane thickness with scattered-light models for edge-on disks suggests a mass on the order of $0.006\,M_{\odot}$. Thus far the disk has not been unambiguously detected in the millimeter continuum, which would allow the mass to be established directly (Bally et al. 1998b). Finally, relatively little envelope material is seen at high latitudes above the 114-426 disk: this could be interpreted as implying that it represents the stage of YSO circumstellar material evolution immediately after IRAS 04302+2247, but may alternatively be more related to environmental effects.

3. HH 30: a prototype disk-jet system

Disks and jets associated with young stars are expected to be oriented perpendicularly, and recent high-resolution images have confirmed this expectation at the sub-arcsecond level. For example, HST images of Haro 6-5B and DG Tauri B show compact bipolar nebula structures and dust lanes several hundred AU in diameter (Krist et al. 1998; Padgett et al. 1999a). The sharpest and most symmetric system is HH 30 (see Fig. 1c; Burrows et al. 1996; Ray et al. 1996), the source of a spectacular jet in the Taurus L 1551 molecular cloud (Mundt et al. 1990).

HH 30 was the first YSO disk in which the vertical structure was clearly resolved. The disk is seen to flare (become thicker) with increasing radial distance, confirming longstanding predictions from disk structure theory and SED fitting (Lynden-Bell and Pringle 1974; Kenyon and Hartmann 1987; Bell et al. 1997). Modelling of the isophotes (Burrows et al. 1996; Wood et al. 1998) indicates that the disk is vertically hydrostatic with a scale height $H = 15\,\mathrm{AU}$ at $r = 100\,\mathrm{AU}$; furthermore Burrows et al. (1996) found that its scale height may flare with radius more rapidly than expected for a steady-state accretion disk. The disk outer radius is 225 AU, with an inclination angle of $\sim 7\,°$.

The disk molecular gas component and its kinematics have been resolved via millimeter interferometry by Stapelfeldt and Padgett (1999), while millimeter continuum measurements have yielded a surprisingly small total disk mass of $\sim 10^{-3}\,M_\odot$ assuming nominal dust properties, similar to the mass derived independently from the HST images. This mass is much less than typically inferred for Herbig-Haro jet sources (Reipurth et al. 1993). Implications are that the HH 30 disk must be largely optically thin to its own emergent thermal-IR radiation, and also that steady accretion would consume the system in less than 0.1 Myr. Apparently therefore, HH 30 represents a young star nearing the end of its disk accretion phase.

4. HK Tau/c: a circumstellar disk in a binary system

High-resolution imaging of the faint companion star to HK Tauri shows it to be a nebulous edge-on disk (Fig. 1d; Koresko 1998; Stapelfeldt et al. 1998), making it the first such object seen in a young binary system. HK Tau/c is very small, with a 1.5 arcsec size corresponding to a disk radius of 105 AU, and an extremely narrow 0.2 arcsec dust lane: objects like HK Tau/c would be difficult to recognize as edge-on disks beyond the nearest star-forming clouds.

Modelling of the isophotes (Stapelfeldt et al. 1998) indicates a disk inclination of $\sim 5\,°$ and a scale height $H = 3.8\,\mathrm{AU}$ at $r = 50\,\mathrm{AU}$, making the disk significantly flatter than that of HH 30. For its estimated age of 0.5 Myr, the disk mass appears to be extremely small: Stapelfeldt et al. (1998) find it to be $10^{-4}\,M_\odot$ ($0.1\,M_{\mathrm{Jup}}$) based on HST optical wavelength observations, while Koresko (1998) derives $10^{-3}\,M_\odot$

from ground-based near-IR speckle holography. With its small apparent mass, 1–10% that of the minimum mass solar nebula, and little evidence for accretion, HK Tau/c may represent a disk which has already been partially dissipated.

The mass and radius of the HK Tau/c disk have likely been reduced by tidal effects of the nearby primary star. However, it will be difficult to evaluate the importance of these perturbations quantitatively until the orbital parameters of the binary are established. Statistically, the physical separation of the two stars is likely to be about twice the projected separation, or 700 AU. This would make the observed disk radius about 15% of the distance between the components, and would require the disk plane to be inclined to the stellar orbit plane. The HK Tauri system therefore provides an interesting case for the application of binary/disk interaction theory (Lubow and Artymowicz, this volume).

B. Silhouette disks around directly visible stars

As discussed above, silhouette disks are seen in projection against a bright background screen. Even when not edge-on, they can still be seen at reasonably high contrast as long as the background illumination is provided by a bright emission line (e.g., from an H II region), since a narrow-band filter can be used to accept all the light from the emission line, while simultaneously suppressing the bulk of the continuum light from the central star. In addition to the edge-on disks seen in the Orion Nebula, others are seen at inclinations which allow their central star to be detected directly (Fig. 2; McCaughrean and O'Dell 1996).

A combination of optical, near-, and mid-IR photometry for the central stars shows that they are typically young (1–2 Myr) and low-mass (0.3–1.5 $M_\odot$), all with excess thermal-IR emission indicating hot dust near the inner edge of the disk (McCaughrean and O'Dell 1996; Hayward and McCaughrean 1997). In this sense, they appear to be counterparts to classical T Tauri stars, although unlike most T Tauri stars, the disks are seen directly and their outer radii accurately determined from the silhouette, with the non-edge-on Orion Nebula silhouette disks ranging in diameter from 50–500 AU.

Since these disks are seen partly face-on, it has been possible to examine their surface density profiles, at least near the edges, and McCaughrean and O'Dell (1996) showed the disks are best fit with an opaque inner section and relatively sharp exponential edge. Since the inner section is highly optically thick, standard radial surface density laws with $\Sigma(r) \propto r^p$ (with p in the range -0.75 to -1.5; Shakura and Sunyaev 1973; Adams, Shu, and Lada 1988) cannot be ruled out there, but the disks do appear to have been truncated at some outer radius. Possible causes include the following:

1. Internal disk evolution

Simple gravity-dominated models show that as circumstellar disks form via inside-out collapse, they comprise two distinct parts, an inner disk, rotating in quasi-equilibrium and an outer component contracting dynamically (Saigo and Hanawa 1998). The presence of a sharp transition zone between the two parts is predicted, and while it is possible that this corresponds to the edges seen in the silhouette images, there appears to be little evidence for more extended infalling envelopes around the Orion disks, which may have been removed by external effects. Also, such a simple model may be significantly modified if magnetic fields play an important role in the collapse.

2. OB star ionizing flux and stellar wind

Near the center of the Orion Nebula, low-mass stars are often accompanied by compact nebulae, externally ionized by the Trapezium OB stars. These so-called 'proplyds' are thought to have disks at their centers (O'Dell et al. 1993; O'Dell and Wong 1996; Bally et al. 1998a; Henney et al. 1996; Johnstone, Hollenbach, and Bally 1998; see also the chapter in this volume by Hollenbach et al.). The silhouette disks are simply thought to be far enough from the OB stars to escape ionization, but it is nevertheless plausible that smaller-scale effects are at work: for example, Orion 121-1925 has a faint tail that points away from the brightest OB star θ^1Ori C, perhaps being driven off by the stellar wind. Such an effect should truncate the disk, although modelling is required to determine the likely profile.

3. Star/disk interactions

The Trapezium Cluster contains many low-mass stars and tidal interactions between a star/disk system and interloper stars should lead to distortion, tidal tails, and truncation of the disk (Heller 1995; Hall, Clarke, and Pringle 1996; Larwood et al. 1996). Models by Hall (1997) show that repeated encounters with stars in a cluster can convert an original power-law radial profile into one with a sharper exponential edge, as observed for the silhouette disks.

A more global form of tidal stripping may truncate a disk at the radius where its Keplerian velocity is of the same order as the cluster velocity dispersion, inasmuch that the latter reflects the general gravitational potential of the cluster. The Keplerian velocities at the outer edges of the silhouettes, calculated from their radii and central stellar masses, are typically ~ 1.5–$2.5\,\mathrm{km\,s^{-1}}$. By comparison, the 3D cluster velocity dispersion is $\sim 4\,\mathrm{km\,s^{-1}}$ (Jones and Walker 1988), and a proper analysis would be required to determine whether or not the field corresponding to that velocity would indeed truncate the disks at the observed radii.

4. Pressure balance

An edge may also be expected when the cold gas in the disk comes into pressure equlibrium with the hot ionized gas of the H II region. Assuming a temperature and density for the ionized gas of 10^4 K and $10^4\,\mathrm{cm}^{-3}$ respectively, the corresponding disk density would be 10^6–$10^7\,\mathrm{cm}^{-3}$ for reasonable disk temperatures of 100–10 K. McCaughrean and O'Dell (1996) show that such a volume density converts to a column density roughly equivalent to an extinction of $A_V \sim 1$ (i.e., as observed at the disk edge), for plausible disk thicknesses.

5. Ram pressure stripping

Finally, a rotating disk translating through the H II region at a few $\mathrm{km\,s^{-1}}$ should be compressed on the side where the rotation and translation velocities are in opposition, and stripped on the side where they combine, leading to truncation and a steady-state asymmetry in the disk. Similar ram pressure stripping are modelled and observed for spiral galaxies (e.g., Kritsuk 1983; Phookun and Mundy 1995).

Most of these effects are external and it is clear that the environment in which stars, disks, and planetary systems form might play a crucial role in defining their parameters (see also Walter et al., this volume). Planets are thought to begin forming within the first 1 Myr or so, and thus it is important to know if the effects of environment at that early stage are important in promoting or retarding their formation. The panoply of destructive effects apparently present in the Orion Nebula might suggest that disks would have a hard time surviving long enough to form planets. However, as Hall (1997) has shown, while repeated star/star encounters in a cluster will sharply truncate the outer edge of a disk, cutting it off from any larger-scale reservoir of material, a significant fraction of the disk material is actually moved *inwards*, piling it up within a few tens of AU, where planets are thought to form. Also, spiral instability waves excited by these close encounters might cause material to accumulate preferentially thus seeding the formation of planets.

To date, the Orion Nebula is the only site where silhouette disks have been seen: surveys in other H II regions and reflection nebulae have so far been unsuccessful (Stapelfeldt et al. 1997). There are two reasons why this might the case: on one hand, emission lines from fainter H II regions or continuum light from reflection nebulae might simply provide insufficient contrast to see a silhouette; on the other, the Orion Nebula might be seen at a special time, when disks around the low-mass stars have only just been uncovered by the OB stars, but have not yet been destroyed by them.

C. Disks seen in the presence of bright starlight

Most disk systems will neither be edge-on nor located in bright H II regions. These systems will typically be viewed at inclinations which allow the relatively bright central star to be seen directly along the line of sight, thus swamping the faint scattered light from the disk. Furthermore, if the disk is not flared, the inner disk may cast the outer regions in shadow.

The detection of a disk in such systems is difficult but not impossible, with a stable, largely symmetric, and well-calibrated PSF the basic requirement. The visibility of the faint disk nebulosity increases rapidly with distance from the central star, and estimates of the detectable disk mass and size completeness curves can be made for a given inclination, using empirical PSFs (Close et al. 1998b). For example, assuming an ISM-like distribution of dust grains (Mathis and Whiffen 1989), Mie scattering calculations show that a $\sim 0.01\,M_{\odot}$ disk at an inclination of 45° is detectable at radii $\gtrsim 1$ arcsec from the central star providing 0.1 arcsec resolution can be achieved. For a fully-sampled pixel scale (e.g., ~ 0.05 arcsec), such a disk has a typical per-pixel surface brightness 10^5 times fainter than the central star. At the 150 pc distance to the nearest star-forming regions, only the largest disks ($\gtrsim 100$ AU radius) have been studied so far: imaging of smaller disks is challenging.

As discussed in the introduction, millimeter interferometry provides an important tool for studying the outer parts of large circumstellar disks, with the advantages that emission from the central star is negligible, and that the gas kinematics can be studied directly. For example, the millimeter emission from GG Tau (Dutrey et al. 1994), GM Aur (Dutrey et al. 1998), DM Tau (Saito et al. 1995; Guilloteau and Dutrey 1998), and UY Aur (Duvert et al. 1998) have all been resolved and found to be consistent with Keplerian disks. HL Tau appears to have signs of rotation as well (Sargent and Beckwith 1991), although infall (Hayashi et al. 1993) and perhaps outflow (Cabrit et al. 1996) have also been observed, underlining how complex the kinematics can be. Since each of these systems are known to have disks in Keplerian rotation with resolved diameters of a few arcseconds, they are natural candidates for direct imaging in light scattered by associated dust. All have been imaged by the HST in the optical and by AO in the near-IR, with HL Tau, GM Aur, GG Tau, and UY Aur all detected. Surprisingly, the DL Tau and DM Tau disks have yet to be seen: it is plausible that the dust in these systems has already condensed to form grains too large ($>10\,\mu$m) to scatter efficiently.

1. HL Tau: a young embedded source

HL Tau is likely the youngest such system. Although the central star is obscured by ~ 24 magnitudes of visual extinction (Stapelfeldt et al. 1995; Beckwith and Birk 1995; Close et al. 1997a), it is not an edge-on system, with inclination estimates varying between 20–40° (cf. Mundy et al. 1996). The large visual extinction is apparently caused by the dusty upper part of the disk/envelope. There is significant infall in the envelope (Hayashi et al. 1993), and a strong 300 km s^{-1} outflow (Mundt et al. 1990); these features, combined with strong emission lines and continuum veiling (Cohen and Kuhi 1979; Basri and Batalha 1990) all attest to the youth of HL Tau. Dereddened near-IR colors suggest a very young ($\sim$0.1 Myr) low-mass ($0.7\,M_\odot$) pre-main sequence (PMS) star (Close et al. 1997a).

HL Tau is unique in that its disk is dense (total mass $\sim 0.1\,M_\odot$) and large ($\sim$ 150 AU radius) enough to be directly resolved in sub-mm and mm continuum emission from dust (Lay et al. 1994; Mundy et al. 1996; Wilner and Lay, this volume). AO imaging at $1.2\,\mu$m with 0.2 arcsec spatial resolution shows a similar extent to that seen in the millimeter continuum (radius $\sim$ 150 AU; position angle $\sim 125°$) with an inclination of $\sim 20°$. Both HST and AO observations detect cavities above and below the disk (Stapelfeldt et al. 1995; Close et al. 1997a), most likely produced by the fast $300\,\mathrm{km\,s^{-1}}$ jet (see Fig. 3a). As these cavities expand, the PMS star should become directly visible in the optical.

2. GM Aur: an older circumstellar disk

The GM Aur disk has been detected by the HST (Stapelfeldt et al. 1997) in the optical and via AO in the near-IR (Close et al. 1998). Compared to HL Tau, GM Aur is a rather evolved T Tauri star with little envelope material visible. Indeed, weaker extinction towards the source and a lack of strong veiling or outflow argue for a more moderate $\sim$ 1 Myr age for the system. The AO images (see Fig. 3b) suggest GM Aur has a $\sim$ 300 AU radius disk, enhanced on its near-side due to forward scattering, while the HST images show a larger radius $\sim$ 450 AU and an inclination of 20–30° from preliminary modelling.

3. GG Tau: a circumbinary disk

Perhaps one of the most interesting surprises resulting from direct imaging of disks was their detection around binary T Tauri stars (see Mathieu et al., this volume. The best known example is GG Tau, where millimeter interferometry revealed a large circumbinary disk in Keplerian rotation, albeit only marginally resolved (Dutrey et al. 1994). AO images at 0.1 arcsec resolution (Fig. 3c; Roddier et al. 1996) show a ring inclined at 55°, and an inner hole with a radius of $\sim$ 190 AU. Scattered-light models of the system have been presented Wood et al. (1999). The inner hole size is some 2.7 times larger than the binary semi-major axis, consistent with models that show that the lower-mass companion in a binary system should eject disk material via tidal effects, clearing such a hole (Artymowicz and Lubow 1995; Lubow and Artymowicz, this volume). The inner hole in a circumbinary disk moves the peak nebular brightness off the central star, suggesting that, in general, it may be relatively easier to detect disks via direct imaging in scattered light in binary systems compared to those around single stars.

Once the inclination of a circumbinary disk is known, and its orientation and velocity profile modeled from the millimeter maps, the total mass of the binary can be estimated: for GG Tau, Dutrey et al. (1994) estimated a total mass of $1.2\,M_\odot$. This can be independently checked by monitoring the relative motion of the two binary stars (separation 0.25 arcsec) via speckle and AO observations (Leinert et al. 1993; Ghez et al. 1993, 1995; Roddier et al. 1996). The presently measured orbital velocity of ~ 1.45 AU/yr (under the assumption that the stars are coplanar with the $35°$ inclination disk), suggests that the binary is close to minimum separation and contains a total mass of $\sim 1.5\,M_\odot$. Distance and velocity uncertainties yield a possible 40% error in this mass estimate, making it consistent with that determined from the millimeter kinematics. Interestingly, both estimates are considerably higher than the masses derived from the stellar fluxes using current PMS evolution models (D'Antona and Mazzitelli 1994; Roddier et al. 1996).

4. UY Aur: a large circumbinary disk

Millimeter interferometry has also revealed a circumbinary disk around UY Aur (Dutrey et al. 1996; Duvert et al. 1998), as also seen via AO imaging (Fig. 3d; Close et al. 1998a). Compared to GG Tau, the UY Aur disk is larger, with an inner hole radius ~ 420 AU. This is unsurprising however, since the UY Aur binary has a larger projected separation of 0.88 arcsec, corresponding to a semi-major axis of ~ 190 AU, and thus the observations confirm the prediction that wider binaries should have larger gaps in their disks.

The millimeter interferometry suggests that the disk gas is in Keplerian rotation around a $1.2\,M_\odot$ binary (Duvert et al. 1998), while the binary orbital motion yields the slightly higher mass of $1.6 \pm 0.5\,M_\odot$. As with GG Tau, the kinematic masses are higher than those derived from stellar fluxes combined with PMS tracks. In both GG Tau and UY Aur, in addition to the large (300–500 AU) circumbinary disks, much smaller (5–10 AU) circumstellar disks must be present around each binary component in order to account for near-IR excesses seen in their SEDs (Close et al. 1998a). Short estimated lifetimes for these inner disks makes it likely that they are replenished via accretion from the outer large circumbinary disks, in line with theoretical expectations (cf. Duvert et al. 1998; Close et al. 1998a; Lubow and Artymowicz, this volume).

Finally, the large size of the UY Aur disk makes it possible to obtain imaging polarimetry, a difficult proposition requiring a stable and sharp PSF (Close et al. 1997b). AO imaging polarimetry with 0.09 arcsec resolution indicates that the light from the UY Aur disk is strongly polarized ($\sim$80%) due to single scattering off mainly small ($< 0.1\,\mu$m) dust grains (Potter et al. 1998). The observed polarization pattern around UY Aur was found to be in good agreement with the dust grains distributed in a disk: other distributions, such as a spherical envelope, can be rejected by comparison with suitable models (Potter et al. 1998).

IV. PHYSICAL PROPERTIES OF DISKS

Models of the distribution of light scattered by circumstellar dust grains for a variety of density distributions have been presented by Whitney and Hartmann (1992, 1993), Fischer, Henning, and Yorke (1996), and Wood et al. (1998). For circumstellar disks, power law formulations are conventionally adopted for the radial dependence of surface density, $\Sigma(r) = \Sigma_0(r/r_0)^p$, and scale height, $H(r) = H_0(r/r_0)^\beta$. A vertically isothermal, pressure-supported disk in a gravitational potential dominated by its central star then follows a density law

$$\rho(r,z) \propto \frac{M_d}{H_0 R_o^2}\left(\frac{r}{r_0}\right)^\alpha \exp(-z^2/2H(r)^2) \tag{1}$$

where r and z are cylindrical coordinates, M_d is the disk mass, R_o is the disk outer radius, $\alpha \equiv p-\beta$, and r_0 is a fiducial radius. Combined with assumptions about the dust opacity for scattering/absorption, the dust albedo, and a scattering phase function, the modelling task is largely reduced to calculation of column density integrals and projection angles, although proper treatment of polarization can add significant complexity. In this section, we discuss the extent to which such modelling of the optical/near-IR observations of disks has succeeded in determining some of their more important physical parameters (see also Wilner and Lay, this volume, for constraints on disk parameters from modeling of millimeter/submillimeter images and visibilities).

A. Outer radius

Observations in scattered light do not necessarily reveal the full radius of the disk, as demonstrated by Orion 114-426, where the polar scattering lobes seen in the near-IR are somewhat smaller than the disk outer radius as seen in silhouette (McCaughrean et al. 1998). Also, the radial extent of a disk traced in molecular line maps made in CO isotopes is generally larger than seen in scattered light (Stapelfeldt and Padgett 1999; Padgett et al. 1999b). In some cases, observations may be insufficiently sensitive to detect faint nebulosity to the full radial extent of the system. Alternatively, outer disk regions can be shadowed by the inner disk if the flaring function turns over (dH/dr becomes negative). Conversely however, the average size of disks seen via scattering or absorption is significantly larger than inferred from modelling of the infrared SEDs (Beckwith et al. 1990).

B. Inclination

Theoretically, an edge-on disk should have bipolar reflection nebulae of equal brightness, while at increasing inclinations, the far side of the disk will appear progressively smaller and fainter than the near side. The inclination of an observed disk can thus be derived by comparison with a grid of models, although this simple trend can break down if significant scattered light from an envelope is present. The inclination derived in this way can be independently checked using measurements of the kinematics in an associated jet, assuming perpendicularity.

C. Mass

In principle, the brightness of the scattered light can be used to estimate the disk mass, but as found for the corresponding absorption in the silhouette disks, very little material is required to account for the observations, due to the large optical depths at optical/IR wavelengths. Thus only lower limits are derived, typically just $\sim 10^{-5} M_\odot$ for the scattered light. However, in an edge-on system, the nebular structure is strongly affected by the total mass in the disk, with the thickness of the central dust lane increasing monotonically with disk mass, as shown in Fig. 4. Thus, high-resolution images of an edge-on disk can be compared with a grid of models to determine its mass. For the two edge-on systems where millimeter continuum observations are currently available, IRAS 04302+2247 and HH 30, the millimeter-derived masses are in reasonable agreement with those obtained from scattered light models, giving some some confidence in the applicability of a disk density law to these systems, and in the current knowledge of dust opacities at optical and millimeter wavelengths.

D. Radial density profile

The radial density distribution is not well determined by observations at wavelengths where disks are optically thick. It is only in the very outermost sections of the silhouette disks, for example, that their structure can be traced, revealing their strongly truncated outer edges (see Section III.B). In HH 30 and HK Tau/c, models using only the nebula light distribution as a constraint suggest a surface density weakly *increasing* with radius, although the same models produce too little extinction to obscure the central star. To reproduce the minimum necessary extinction, a radially decreasing surface density is required, but since p is seen to be strongly degenerate with the scale height index β, only a weak conclusion can be drawn, namely that $p < -0.3$ in both systems.

E. Vertical structure and its radial dependence

In edge-on systems, gradients in the nebular brightness adjacent to the dark lane allow the scale height near the disk outer radius to be derived. This parameter is interesting since it can be directly related to the local temperature in a disk which is vertically hydrostatic; its radial variation is diagnostic of the radial temperature structure. In addition, changes in the vertical distribution of scattering dust grains may accompany the initial stages of particle growth which lead to planetesimal formation.

Burrows et al. (1996) and Wood et al. (1998) independently derived identical values for the reference scale height, H_0, in the HH 30 disk, and while a weak coupling of H_0 with other model parameters is seen, the systematic uncertainty introduced is less than 20%. Unfortunately, these modelling efforts have also shown that the radial dependence of scale height (the exponent β) cannot be uniquely determined from a single image, since the outer disk, where the scale height is largest, obscures both the central star and the inner disk from direct view. Thus the vertical profile is not observed over a large enough range of radii to allow β to be uniquely solved for, although in the future, it may be possible to solve for β uniquely via combined modelling of multiwavelength image data and the disk SED.

F. Circumstellar dust properties

When comparing the models of the scattered light nebulae associated with circumstellar disks with the observations, the assumed dust grain properties can also be tested. For example, it is widely expected that grain growth will occur in dense circumstellar regions, and this growth might be enough to affect the nebula models. As a starting point, most authors use the properties of normal interstellar grains, which are well-characterized both observationally and theoretically.

In general, any distribution of circumstellar dust grains will have a mix of small and large grains. If all these grains were homogeneous spheres with radii in the range 0.01–1 μm, exact Mie scattering theory (e.g., Bohren and Huffman 1983) could be used to calculate their scattering properties in in the optical/near-IR wavelength regime. However, it is likely that real circumstellar grains have more complex, possibly fractal geometries and consist of an aggregate of different materials (Ossenkopf 1991; Kozasa et al. 1992), making them hard to model. Fortunately, Rouleau (1996) has recently shown that the convoluted surface of such a grain can be well approximated by a spherical grain with the same total surface area. This presumably accounts for the success of Mathis and Whiffen (1989) in reproducing the observed ISM extinction curve from UV to far-IR wavelengths (cf. Mathis 1990) using a simple power-law distribution of spherical grains, combined with a 'mix' of different dielectric constants of various minerals and vacuum, produce a single effective dielectric constant.

Close et al. (1998a) created a similar recipe for circumstellar grains, using a composition of amorphous carbon, graphite, and silicates, and 80% vacuum by volume (similar to model A of Mathis and Whiffen 1989). A power-law distribution of radii was assumed, with $n(a) = Ca^{-\eta}$ and $n(a)\,da$ equal to the number density of grains per hydrogen atom with radii between a and da. The size distribution has upper and lower limits at $a_{\rm max}$ and $a_{\rm min}$ respectively.

Close et al. (1998a) used this grain prescription in their models for the scattered light seen in the circumbinary disks around GG Tau and UY Aur systems where the inclination was well-established from the millimeter kinematics. They found the best results were obtained using a power-law index of $\eta = 4.7$, and radii ranging from 0.03 up to 0.5–0.6 μm, i.e., similar to ISM grains. A significant population of grains with radii >0.6 μm was found to be unlikely, since such large grains would increase the contrast between the near and far sides of the disk to levels higher than observed. Burrows et al. (1996) and Stapelfeldt et al. (1998) derived similar results for their models of the HH 30 and HK Tau/c edge-on disks, although the presence of a population of somewhat larger (~1 μm) grains was implied based on the apparently enhanced forward scattering at 0.8 μm wavelength. Nevertheless, the larger millimeter-sized grains inferred by millimeter observations apparently do not play a major role in the scattering process: it is possible that they may have sunk to the central (optically thick) plane of the disks, remaining hidden from view in scattered light, but nevertheless still dominating the millimeter continuum emission.

VI. FUTURE DEVELOPMENTS

Almost all of the results presented in this review have been obtained since the Protostars and Planets III meeting in 1990, and clearly, before the next meeting in the series, substantial progress will be made in studying the most important phases in the formation and evolution of young circumstellar disks and proto-planetary systems.

Foremost is the need to find more examples of disks around young stellar objects at all evolutionary stages, by continuing surveys of nearby dark clouds and H II regions. Existing techniques will be used to the full, including AO on the ground and the HST in space. The next HST servicing mission will see the installation of the wide-field fully-sampled Advanced Camera for Surveys at optical wavelengths and the possible return to operation of NICMOS in the near-IR.

Second, improvements in angular resolution are required to allow more detailed studies of nearby sources, and to extend the surveys to encompass the more distant star-forming regions with reasonable linear resolution. In the near-term, this will be achieved on the ground by equipping the 8–10 m class telescopes with AO systems; in the longer-term, significant gains will be made by the passively-cooled IR-optimized Next Generation Space Telescope (NGST) and through multi-telescope optical/IR interferometry, using, for example, the Keck, VLTI, and LBT interferometers on the ground, and SIM in space. Malbet et al. (1998) have very recently shown the way forward in this regard, using the Palomar Testbed Interferometer to resolve thermal emission from a disk around FU Ori at near-IR wavelengths, at spatial scales around 4 milliarcsec or just 2 AU at 450 pc.

Finally, there is a strong case for increased-contrast imaging, in order to study low-surface brightness scattered light in the presence of a bright central star. There are several known examples of YSOs with disks which have been resolved via millimeter interferometry, and yet which show just bare PSFs in HST and/or AO images at optical/near-IR wavelengths. These systems, including DL Tau, DM Tau, CY Tau, V 892 Tau, MWC 480, LkCa 15, and AS 209, clearly have disks, but current optical/near-IR instrumentation is simply not up to the contrast challenge. Future ameliorating developments will include improved forms of coronagraphy and optical/IR nulling interferometry on the ground and in space.

Acknowledgements: The research described in this paper was carried out in part by the Jet Propulsion Laboratory, California Institute of Technology, under a contract with the National Aeronautics and Space Administration.

Figure 1. Continuum HST images of four edge-on disks, all plotted at the same equivalent linear scale and orientation for direct comparison. IRAS 04302+2247 (top left; Padgett et al. 1999a) and Orion 114-426 (top right; McCaughrean et al., in preparation) are shown as near-infrared truecolor JHK composites. Both HH 30 (bottom left; Burrows et al. 1996) and HK Tau/c (bottom right; Stapelfeldt et al. 1998) are shown as optical pseudocolor RI composites. Each panel is 1200 AU square and all intensities are logarithmically scaled.

Figure 2. HST images of four silhouette disks in the Orion Nebula. From left to right: Orion 218-354, 167-231, 121-1925, and 183-405. All are seen against the nebular Hα background with either the Wide Field Camera or Planetary Camera in these relatively shallow survey images. Each panel is 2.0 arcsec or 900 AU square, cf. the 60 AU diameter of the Solar System. From McCaughrean and O'Dell (1996).

Figure 3. Four circumstellar disks detected in scattered light. The HL Tau image (top left) is a composite of an HST R-band image as blue (from Stapelfeldt et al. 1995), and AO images at J and H as green and red respectively (from Close et al. 1997a). The green extension is likely infrared light scattered off the front surface of the disk. Both GM Aur (top right) and GG Tau (bottom left) are represented with J-band AO images: note that the GG Tau logarithmic intensity scale is wrapped in order to show both the faint nebulosity and the fully-resolved central binary (from Roddier et al. 1996). UY Aur (lower right) is shown as a composite JHK (as blue, green, red) AO image (from Close et al. 1998a). This circumbinary disk is somewhat closer to edge-on than that seen in GG Tau, and thus emission from the near-side of the disk is strongly scattered into the line-of-sight.

Figure 4. Scattering models at $\lambda = 0.8\,\mu$m for optically thick, nearly edge-on circumstellar disks. The increase in apparent dust lane thickness as a function of disk mass is illustrated by models with $10^{-6}\,M_\odot$ (top left), $3 \times 10^{-5}\,M_\odot$ (top right), $10^{-3}\,M_\odot$ (lower left), and $3 \times 10^{-2}\,M_\odot$ (lower right) of gas and dust.

REFERENCES

Adams, F. C., Shu, F. H., and Lada, C. J 1988. The disks of T Tauri stars with flat infrared spectra. *Astrophys. J.* 326:865–883.

Artymowicz, P., and Lubow, S. H. 1996. Mass flow through gaps in circumbinary disks. *Astrophys. J. (Letters)* 467:L77–L80.

Artymowicz, P., and Lubow, S. H. 1995. Interaction of young binaries with protostellar disks. In *Disks and outflows around young stars*, eds. S. V. W. Beckwith, J. Staude, A. Quetz, and A. Natta, (Heidelberg: Springer), pp. 115–131.

Bally, J., Sutherland, R. S., Devine, D., and Johnstone, D. 1998a. Externally illuminated young stellar environments in the Orion Nebula: Hubble Space Telescope Planetary Camera and ultraviolet observations. *Astron. J.* 116:293–321.

Bally, J., Testi, L., Sargent, A. I., & Carlstrom, J. 1998b, Disk mass limits and lifetimes of externally irradiated young stellar objects embedded in the Orion Nebula. *Astron. J.*, 116:854–859.

Basri, G., and Batalha, C. 1990. Hamilton echelle spectra of young stars. I—Optical veiling *Astrophys. J.* 363:654–669.

Beckwith, S. V. W., and Birk, C. C. 1995. Vertical structure in HL Tauri. *Astrophys. J. (Letters)* 449:L59–L63.

Beckwith, S. V. W., Koresko, C. D., Sargent, A. I., and Weintraub, D. A. 1989. Tomographic imaging of HL Tauri. *Astrophys. J.* 343:393–399.

Beckwith, S. V. W., and Sargent, A. I. 1993. The occurrence and properties of disks around young stars. In *Protostars & Planets III*, eds. E. H. Levy and J. I. Lunine, (Tucson: Univ. Arizona Press), pp. 521–541.

Beckwith, S. V. W. & Sargent, A. I. 1996. Circumstellar disks and the search for neighbouring planetary systems. *Nature* 383:139–144.

Beckwith, S. V. W., Sargent, A. I., Güsten, R., & Chini, R. 1990. A survey for circumstellar disks around young stellar objects. *Astron. J.* 99:924–945.

Beckwith, S. V. W., Skrutskie, M. F., Zuckerman, B., and Dyck, H. M. 1984, Discovery of solar sytem-size halos around young stars. *Astrophys. J.* 287:793–800.

Bell, K. R., Cassen, P. M., Klahr, H. H., and Henning, T. 1997. The structure and appearance of protostellar accretion disks: limits on disk flaring. *Astrophys. J.* 486:372–387.

Bohren, C. F., and Huffman, D. R. 1983. *Absorption and Scattering of*

Light by Small Particles, (New York: John Wiley & Sons)

Burrows, C. J., Stapelfeldt, K. R., Watson, A. M., Krist, J. E., Ballester, G. E., Clarke, J. T., Crisp, D., Gallagher, J. S., III, Griffiths, R. E., Hester, J. J., Hoessel, J. G., Holtzman, J. A., Mould, J. R., Scowen, P. A., Trauger, J. T., and Westphal, J. A. 1996. Hubble Space Telescope observations of the disk and jet of HH 30. *Astrophys. J.* 473:437–451.

Cabrit, S., Guilloteau, S., André, P., Bertout, C., Montmerle, T., and Schuster, K. 1996. Plateau de Bure observations of HL Tauri: outflow motions in a remnant circumstellar envelope. *Astron. Astrophys.* 305:527–540.

Chen, H., Bally, J., O'Dell, C. R., McCaughrean, M. J., Thompson, R. I., Rieke, M., Schneider, G., and Young, E. T. 1998. 2.12 μm molecular hydrogen emission from circumstellar disks embedded in the Orion Nebula. *Astrophys. J. (Letters)* 492:L173–L176.

Close, L., Dutrey, A., Roddier, F., Guilloteau, S., Roddier, C., Northcott, M., Ménard, F., Duvert, G., Graves, J. E., and Potter, D. 1998a. Adaptive optics imaging of the circumbinary disk around the T Tauri binary UY Aur: Estimates of the binary mass and circumbinary dust grain size distribution. *Astrophys. J.* 499:883–888.

Close, L., Roddier, F., Hora, J. L., Graves, J. E., Northcott, M., Roddier, C., Hoffman, W. F., Dayal, A., Fazio, G. G., and Deutsch, L. K. 1997a. Adaptive optics infrared imaging polarimetry and optical HST imaging of Hubble's variable nebula (R Monocerotis/NGC 2261): a close look at a very young active Herbig Ae/Be star. *Astrophys. J.* 489:210–221.

Close, L., Roddier, F., Northcott, M. J., Roddier, C., and Graves, J. E. 1997b. Adaptive optics 0.2 arcsec resolution infrared images of HL Tau: direct images of an active accretion disk around a protostar. *Astrophys. J.* 478:766–777.

Close, L. M., Roddier, F. J., Roddier, C. A., Graves, J. E.Northcott, M. J., Northcott, M. J., & Potterm D. 1998b. Scientific Results From the University of Hawaii Adaptive Optics Program. In *Adaptive optical systems technologies*, Proc. SPIE 3353, eds. D. Bonaccini & R. K. Tyson, pp. 406-416

Cohen, M., and Kuhi, L. V. 1979. Observational studies of pre-main-sequence evolution. *Astrophys. J. Suppl. Ser.* 41:743–843.

D'Antona, F., and Mazzitelli, I. 1994. New pre-main-sequence tracks for M less than or equal to 2.5 solar mass as tests of opacities and convection model. *Astrophys. J. Suppl. Ser.* 90:467–500.

Dutrey, A., Guilloteau, S., Duvert, G, Prato, L, Simon, M., Schuster, K., and Ménard, F. 1996. Dust and gas distribution around T Tauri stars in Taurus-Auriga. I. Interferometric 2.7mm continuum and ^{13}CO J=1–0 observations. *Astron. Astrophys.* 309:493–504.

Dutrey, A., Guilloteau, S., Prato, L., Simon, M., Duvert, G., Schuster, K., and Ménard, F. 1998. CO study of the GM Aurigae Keplerian disk. *Astron. Astrophys.* 338:L63–L66.

Dutrey, A., Guilloteau, S., and Simon, M. 1994. Images of the GG Tauri rotating ring. *Astron. Astrophys.* 286:149–159.

Duvert, G., Dutrey, A., Guilloteau, S., Ménard, F., Schuster, K., Prato, L., and Simon, M. 1998. Disks in the UY Aurigae binary. *Astron. Astrophys.* 322:867–874.

Falcke, H., Davidson, K., Hofmann, K.-H., and Weigelt, G. 1996. Speckle-masking imaging polarimetry of η Carinae: evidence for an equatorial disk. *Astron. Astrophys.* 306:L17–L20.

Fischer, O., Henning, T., and Yorke, H. W. 1996. Simulation of polarization maps. II. The circumstellar environment of pre-main sequence objects. *Astron. Astrophys.* 308:863–885.

Ghez, A. M., Neugebauer, G., and Matthews, K. 1993. The multiplicity of T Tauri stars in the star forming regions Taurus-Auriga and Ophiuchus-Scorpius: a 2.2 μm speckle imaging survey. *Astron. J.* 106:2005–2023.

Ghez, A. M., Weinberger, A. J., Neugebauer, G., Matthews, K., and McCarthy, D. W., Jr. 1995. Speckle imaging measurements of the relative tangential velocities of the components of T Tauri binary stars. *Astron. J.* 110:753–765.

Graves, J. E., Northcott, M. J., Roddier, F. J., Roddier, C. A., & Close, L. M. 1998. First Light for Hokupa'a: 36-element Curvature AO system at the University of Hawaii. In *Adaptive optical systems technologies*, Proc. SPIE 3353, eds. D. Bonaccini & R. K. Tyson, pp. 34-44.

Guilloteau, S., and Dutrey, A. 1998. Physical parameters of the Keplerian protoplanetary disk of DM Tauri. *Astron. Astrophys.* 339:467–476.

Guilloteau, S., Dutrey, A., and Gueth, F. 1997. Disks and outflows as seen from the IRAM interferometer. In *Herbig-Haro flows and the birth of stars*, eds. B. Reipurth and C. Bertout, proc. IAU Symposium 182, (Dordrecht: Kluwer) pp. 365–380.

Hall, S. M. 1997. The energetics of star-disc encounters and the disc density profiles. PhD thesis, University of Cambridge.

Hall, S. M., Clarke, C. J., and Pringle, J. E. 1996. Energetics of star-disc encounters in the non-linear regime. *Mon. Not. R. astr. Soc.* 278:303–320.

Hayashi, M., Ohashi, N., and Miyama, S. M. 1993. A dynamically accreting gas disk around HL Tauri. *Astrophys. J. (Letters)* 418:L71–L74.

Hayward, T. L., and McCaughrean, M. J. 1997. A search for thermal infrared emission from three silhouette disks in Orion. *Astron. J.* 113:346–353.

Heller, C. H. 1995. Encounters with protostellar disks. II. Disruption and binary formation. *Astrophys. J.* 455:252–259.

Henney, W. J., Raga, A. C., Lizano, S., and Curiel, S. 1996. A two-wind interaction model for proplyds. *Astrophys. J.* 465:216–230.

Jayawardhana, R., Fisher, S., Hartmann, L., Telesco, C., Piña, R., and Fazio, G. 1998. A dust disk surrounding the young star HR 4796A. *Astrophys. J. (Letters)* 503:L79–L82.

Johnstone, D., Hollenbach, D., and Bally, J. 1998. Photoevaporation of disks and clumps by nearby massive stars: application to disk destruction in the Orion Nebula. *Astrophys. J.* 499:758–776.

Jones, B. F., and Walker, M. F. 1998. Proper motions and variabilities of stars near the Orion Nebula. *Astron. J.* 95:1755–1782.

Jura, M., Malkan, M., White, R., Telesco, C., Pina, R., and Fisher, R. S. 1998. A protocometary cloud around HR 4796A? *Astrophys. J.* 505:897–902.

Kalas, P. 1996. A coronagraphic survey for circumstellar disks around main sequence and pre-main sequence stars. PhD thesis, University of Hawaii.

Kalas, P., and Jewitt, D. 1996. The detectability of β Pic-like circumstellar disks around nearby main sequence stars. *Astron. J.* 111:1347–1355.

Kenyon, S. J., and Hartmann, L. 1987. Spectral energy distributions of T Tauri stars—disk flaring and limits on accretion. *Astrophys. J.* 323:714–733.

Kitamura, Y., Saito, M., Kawabe, R., and Sunada, K. 1997. NMA imaging of envelopes and disks around low mass protostars and T Tauri stars. In *Herbig-Haro flows and the birth of stars*, eds. B. Reipurth and C. Bertout, proc. IAU Symposium 182, (Dordrecht: Kluwer) pp. 381–390.

Koerner, D. W. 1997. Analogs of the early solar system. In *Planetary and Interstellar Processes Relevant to the Origins of Life*, ed. D. C. B. Whittet, (Dordrecht: Kluwer), pp. 157–184.

Koerner, D. W., Ressler, M. E., Werner, M. W., and Backman, D. E. 1998. Mid-infrared imaging of a circumstellar disk around HR 4796: mapping the debris of planetary formation. *Astrophys. J. (Letters)* 503:L83–L87.

Koerner, D. W., and Sargent, A. I. 1995. Imaging the small-scale circumstellar gas around T Tauri stars. *Astron. J.* 109:2138–2145.

Kozasa, T., Blum, J., Okamoto, H., and Mukai, T. 1993. Optical properties of dust aggregates. II. Angular dependence of scattered light. *Astron. Astrophys.* 276:278–288.

Koresko, C. D. 1998. A circumstellar disk in a pre-main sequence binary star. *Astrophys. J. (Letters)*, 507:145–148.

Krist, J. E., Stapelfeldt, K. R., Burrows, C. J., et al. 1998. Hubble Space Telescope WFPC2 imaging of FS Tauri and Haro 6-5B. *Astrophys. J.* 501:841–852.

Kritsuk, A. G. 1983. Dynamics of the sweeping of interstellar clouds from a rotating galaxy as it moves in the intergalactic medium. *Astrophysics* 19:263–270.

Larwood, J., Nelson, R. P., Papaloizou, J. C. B., and Terquem, C. 1996. The tidally induced warping, precession and truncation of accretion discs in binary systems: three-dimensional simulations *Mon. Not. R. astr. Soc.* 282:597–613.

Lay, O. P., Carlstrom, J. E., Hills, R. E., and Phillips, T. G. 1994. Protostellar accretion disks resolved with the JCMT–CSO interferometer. *Astrophys. J. (Letters)* 434:L75–L78.

Leinert, Ch., Zinnecker, H., Weitzel, N., Christou, J., Ridgway, S. T., Jameson, R., Haas, M., and Lenzen, R. 1993. A systematic approach for young binaries in Taurus. *Astron. Astrophys.* 278:129–149.

Lucas, P. W., and Roche, P. F. 1997. Butterfly star in Taurus: structures of young stellar objects. *Mon. Not. R. astr. Soc.* 286:895–919.

Lynden-Bell, D., and Pringle, J. E. 1974. The evolution of viscous discs and the origin of nebular variables. *Mon. Not. R. astr. Soc.* 168:603–638.

Malbet, F., Berger, J.-P., Colavita, M. M., Koresko, C. D., Beichman, C., Boden, A. F., Kulkarni, S. R., Lane, B. F., Mobley, D. W., Pan, X. P., Shao, M., Van Belle, G. T., and Wallace, J. K. 1998. FU Orionis resolved by infrared long-baseline interferometry at a 2 AU scale. *Astrophys. J. (Letters)* 507:L149–L152.

Mathis, J. S. 1990. Interstellar dust and extinction. *Ann. Rev. Astron. Astrophys.* 28:37–70.

Mathis J. S., and Whiffen G. 1989. Composite interstellar grains. *Astrophys. J.* 341:808–822.

McCaughrean, M. J., Chen, H., Bally, J., Erickson, E., Thompson, R. I., Rieke, M., Schneider, G., Stolovy, S., and Young, E. T. 1998. High-resolution near-infrared imaging of the Orion 114-426 silhouette disk. *Astrophys. J. (Letters)* 492:L157–L161.

McCaughrean, M. J., and O'Dell, C. R. 1996. Direct imaging of circumstellar disks in the Orion Nebula. *Astron. J.* 111:1977–1986.

McCaughrean, M. J., Rayner, J. T., Zinnecker, H., & Stauffer, J. R. 1996. Circumstellar disks in the Trapezium Cluster. In *Disks and outflows around young stars*, eds. S. V. W. Beckwith, J. Staude, A. Quetz, and A. Natta, (Heidelberg: Springer), pp. 33–43.

Mundt, R., Bührke, T., Solf, J., Ray, T. P., and Raga, A.C. 1990. Optical jets and outflows in the HL Tauri region. *Astron. Astrophys.* 232:37–61.

Mundy, L. G., Looney, L. W., Erickson, W., Grossman, A., Welch, W. J., Forster, J. R., Wright, M. C. H., Plambeck, R. L., Lugten, J., and Thornton, D. D. 1996. Imaging the HL Tauri disk at

$\lambda = 2.7$ millimeters with the BIMA array. *Astrophys. J. (Letters)* 464:L169–L173.

O'Dell, C. R., and Wen, Z. 1994. Postrefurbishment mission Hubble Space Telescope images of the core of the Orion Nebula: proplyds, Herbig-Haro objects, and measurements of a circumstellar disk. *Astrophys. J.* 436:194–202.

O'Dell, C. R., Wen, Z., and Hu, X. 1993. Discovery of new objects in the Orion Nebula on HST images—shocks, compact sources, and protoplanetary disks. *Astrophys. J.* 410:696–700.

O'Dell, C. R., and Wong, S.-K. 1996. Hubble Space Telescope mapping of the Orion Nebula. I. A survey of stars and compact objects. *Astron. J.* 111:846–855.

Ossenkopf, V. 1991. Effective-medium theories for cosmic dust grains. *Astron. Astrophys.* 251:210–219.

Osterbart, R., Langer, N., and Weigelt, G. 1997. High-resolution imaging of the bipolar nebula Red Rectangle: evidence for unstable mass transfer in a close binary system. *Astron. Astrophys.* 325:609–612.

Padgett, D. L., Brander, W., Stapelfeldt, K. R., and Koerner, D. 1999b. Anatomy of a butterfly: disk structure models for IRAS 04302+2247. In preparation.

Padgett, D. L., Brandner, W., Stapelfeldt, K. R., Strom, S. E., Koerner, D., and Terebey, S. 1999a. HST/NICMOS imaging of disks and envelopes around very young stars. *Astron. J.*, submitted.

Phookun, B., and Mundy, L. G. 1995. NGC 4654: A Virgo cluster spiral interacting with the intracluster medium. *Astrophys. J.* 453:154–161.

Potter, D. E., Close, L. M., Roddier, F., Roddier, C., Graves, J. E., and Northcott, M. 1998. The first resolved polarimetry map of a circumbinary disk. *Astrophys. J. (Letters)*, submitted.

Ray, T. P., Mundt, R., Dyson, J. E., Falle, S. A. E. G., and Raga, A. 1996. HST observations of jets from young stars. *Astrophys. J. (Letters)* 468:L103–L106.

Reipurth, B., Chini, R., Krugel, E., Kreysa, E., and Seivers, A. 1993. Cold dust around Herbig-Haro energy sources—a 1300 micron survey. *Astron. Astrophys.* 273:221–238.

Roddier, C., Roddier, F., Northcott, M. J., Graves, J. E., and Jim, K. Adaptive optics imaging of GG Tauri: optical detection of the circumbinary ring. *Astrophys. J.* 463:326–335.

Rouleau, F. 1996. Electromagnetic scattering by compact clusters of spheres. *Astron. Astrophys.* 310:686–698.

Saigo, K., and Hanawa, T. 1998. Similarity solution for formation of a circumstellar disk through the collapse of a flattened rotating cloud. *Astrophys. J.* 493:342–350.

Saito, M., Kawabe, R., Ishiguro, M., Miyama, S. M., Hayashi, M., Handa, T., Kitamura, Y., and Omodaka, T. 1995. Aperture synthesis ^{12}CO and ^{13}CO observations of DM Tauri: 350 AU radius circumstellar gas disk. *Astrophys. J.* 453:384–392.

Sargent, A. I., and Beckwith, S. V. W. 1991. The molecular structure around HL Tauri. *Astrophys. J. (Letters)* 382:L31–L35.

Shakura, N. I., & Sunyaev, R. A. 1973. Black holes in binary systems. Observational appearance. *Astron. Astrophys.* 24:337–355.

Schneider, G., Smith, B. A., Becklin, E. E., Koerner, D. W., Meier, R., Hines, D. C., Lowrance, P. J., Terrile, R. J., Thompson, R. I., & Rieke, M. 1999. NICMOS imaging of the HR 4796A circumstellar disk. *Astrophys. J. (Letters)* 513:L127–L130.

Smith, B. A., Fountain, J. W., and Terrile, R. J. 1992. An optical search for Beta Pictoris-like disks around nearby stars. *Astron. Astrophys.* 261:499–502.

Smith, B. A., and Terrile, R. J. 1984. A circumstellar disk around Beta Pictoris. *Science* 226:1421–1424.

Stapelfeldt, K. R., Burrows, C. J., Krist, J. E., Trauger, J. T., Hester, J. J., Holtzmann, J. A., Ballester, G. E., Casertano, S., Clarke, J. T., Crisp, D., Evans, R. W., Gallagher, J. S., III, Griffiths, R. E., Hoessel, J. G., Mould, J. R., Scowen, P. A., Watson, A. M., and Westphal, J. A. 1995. WFPC2 imaging of the circumstellar nebulosity of HL Tauri. *Astrophys. J.* 449:888–893.

Stapelfeldt K. R., Burrows, C. J., Krist, J. E., and the WFPC2 Science Team 1997. Hubble Space Telescope imaging of the disks and jets of Taurus young stellar objects. In *Herbig-Haro Flows and the Birth of Stars* eds. B. Reipurth and C. Bertout, IAU Symposium 182 (Dordrecht: Kluwer), pp. 355–364.

Stapelfeldt, K. R., Krist, J. E., Ménard, F., Bouvier, J., Padgett, D. L., and Burrows, C. J. 1998. An edge-on circumstellar disk in the young binary system HK Tauri. *Astrophys. J. (Letters)* 502:L65–L68..

Stapelfeldt, K. R., and Padgett, D. L. 1999. OVRO millimeter array observations of the HH 30 circumstellar disk. In preparation.

Stapelfeldt, K. R., Sahai, R., Werner, M., and Trauger, J. 1997. An HST imaging search for circumstellar matter in young nebulous clusters. In *Planets beyond the Solar System and the next generation of space missions* ed. D. R. Soderblom, ASP conference series, vol. 119, pp. 131–134.

Whitney, B. A., and Hartmann, L. 1992. Model scattering envelopes of young stellar objects. I—Method and application to circumstellar disks. *Astrophys. J.* 395:529–539.

Whitney, B. A., and Hartmann, L. 1993. Model scattering envelopes of young stellar objects. II—Infalling envelopes. *Astrophys. J.* 402:605–622.

Wood, K., Crosas, M., and Ghez, A. M. 1999. GG Tauri's circumbinary disk: models for near-infrared scattered light images and molecular line profiles. *Astrophys. J.*, submitted.

Wood, K., Kenyon, S. J., Whitney, B., and Turnbull, M. 1998. Optical and near-infrared model images of circumstellar environments of classical T Tauri stars. *Astrophys. J.* 497:404–418.

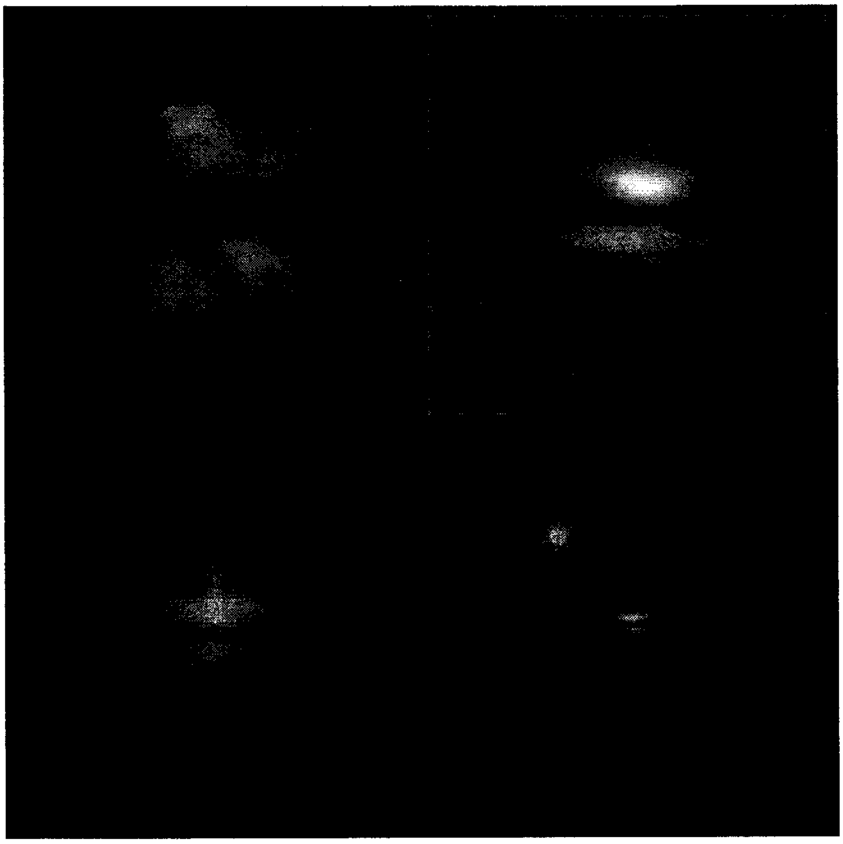

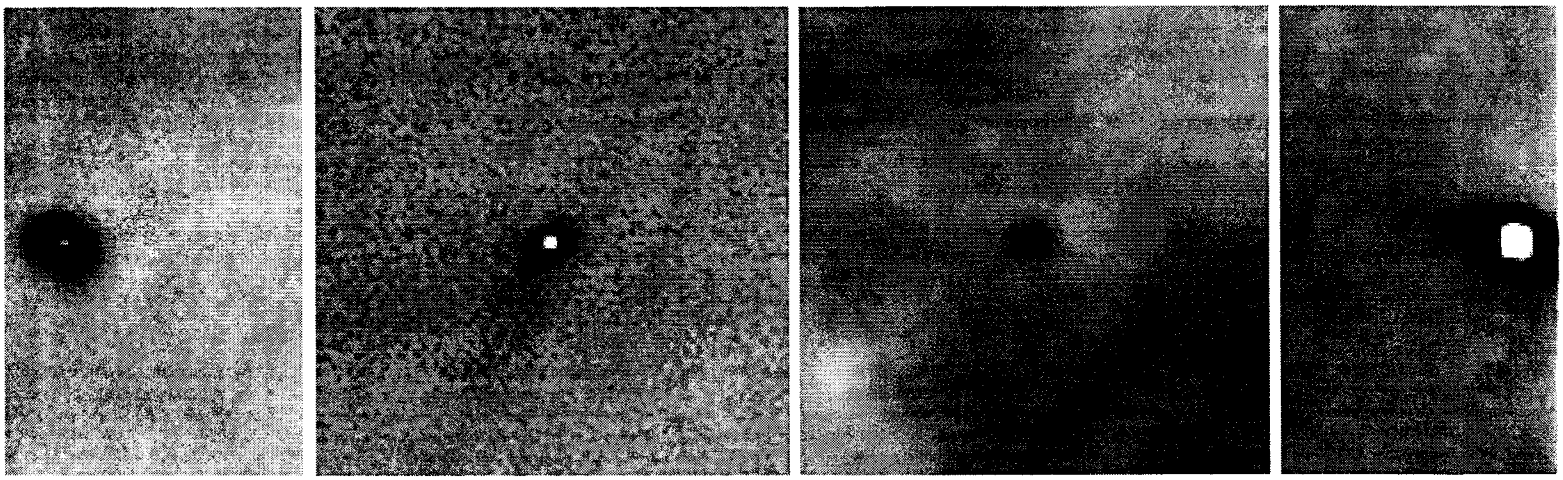

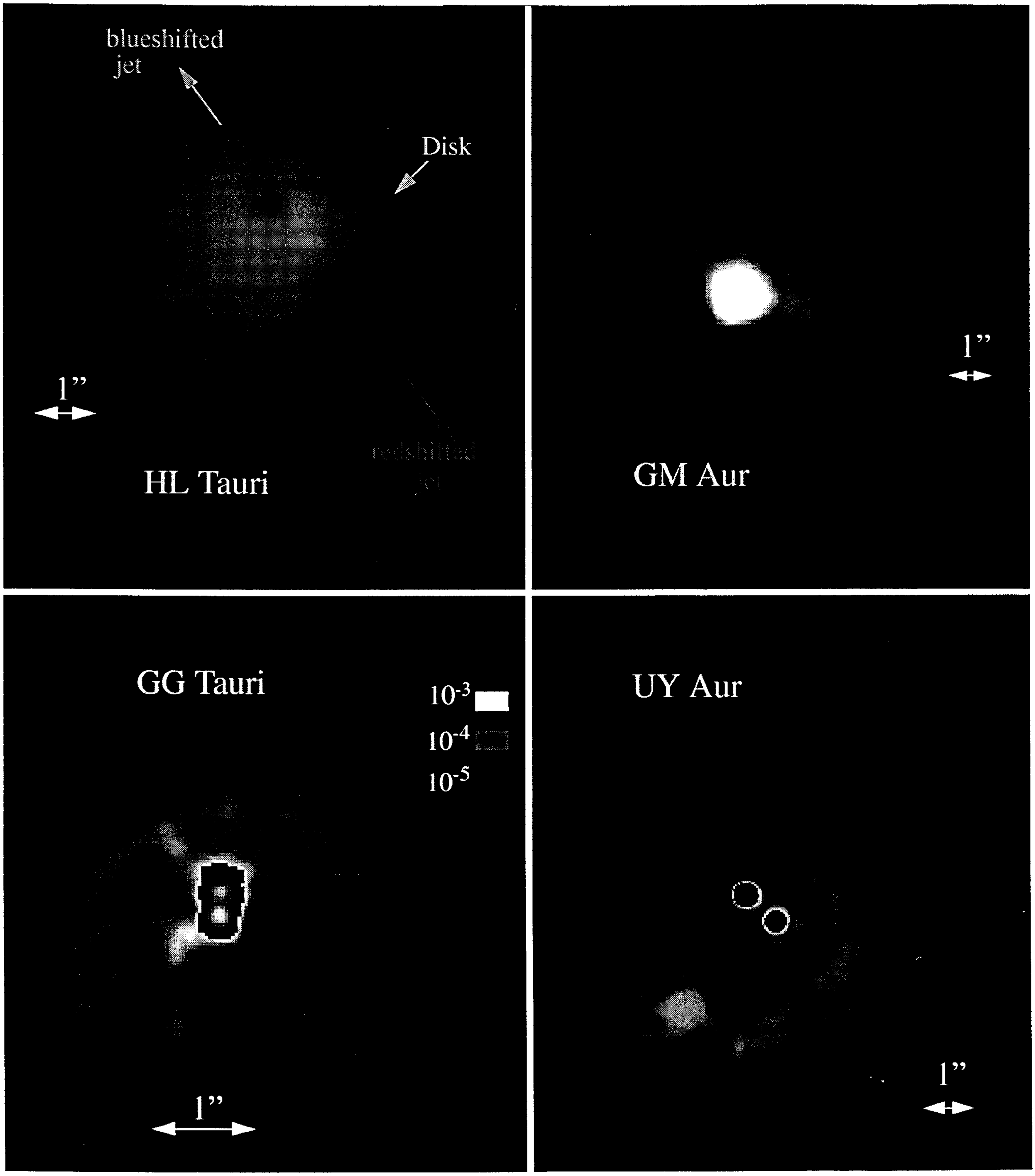

blueshifted
jet
Disk
1"
redshifted
jet
HL Tauri
GM Aur
1"
GG Tauri
10^{-3}
10^{-4}
10^{-5}
1"
UY Aur
1"